1-3-2016

Multi-layered collagen-based scaffolds for osteochondral defect repair in rabbits.

Tanya J. Levingstone
Royal College of Surgeons in Ireland, tanyalevingstone@rcsi.ie

Emmet Thompson
Royal College of Surgeons in Ireland, ethompson@rcsi.ie

Amos Matsiko
Royal College of Surgeons in Ireland, amosmatsiko@rcsi.ie

Alexander Schepens
AZ Sint-Lucas Hospital, Ghent

John Patrick Gleeson
The Royal College of Surgeons in Ireland, johngleeson@rcsi.ie

See next page for additional authors

Citation

Levingstone TJ, Thompson E, Matsiko A, Schepens A, Gleeson JP, O'Brien FJ. Multi-layered collagen-based scaffolds for osteochondral defect repair in rabbits. Acta Biomaterialia. 2016;32:149-60.

Authors
Tanya J. Levingstone, Emmet Thompson, Amos Matsiko, Alexander Schepens, John Patrick Gleeson, and Fergal O'Brien

Multi-Layered Collagen-Based Scaffolds Can Direct Host Stem Cell Differentiation to Achieve Osteochondral Defect Repair in Rabbits

Authors:

*Tanya J. Levingstone, BEng, MSc, PhD [1,2,3]

*Emmet Thompson, MD, PhD [1,2,3]

Amos Matsiko, MEng, PhD [1,2,3]

Alexander Schepens, MD[4]

John P. Gleeson, BA BAI, PhD, MIEI [1,2,3,5]

Fergal J. O'Brien, BA, BAI, PhD, FAS, CEng, FIEI [1,2,3]

* both authors contributed equally to the work

Affiliations:

[1] Tissue Engineering Research Group, Dept. of Anatomy, Royal College of Surgeons in Ireland, 123 St. Stephen's Green, Dublin 2, Ireland.

[2] Trinity Centre for Bioengineering, Trinity College Dublin ,Dublin 2, Ireland

[3] Advanced Materials and Bioengineering Research (AMBER) Centre, RCSI & TCD

[4] Department of Orthopaedic Surgery, AZ Sint-Lucas Hospital, Ghent, Belgium

[5] SurgaColl Technologies Ltd., Invent Centre, Dublin City University, Dublin, Ireland.

Name of the institution where work was completed:

Royal College of Surgeons in Ireland

Corresponding Author:

Prof. Fergal O'Brien,

Department of Anatomy,

Royal College of Surgeons in Ireland,

123 St. Stephen's Green,

Telephone Number: +353 (0)1-402-2149

FAX Number: +353(0)1-402-2355

Email:fjobrien@rcsi.ie

Abstract:

Identification of a suitable treatment for osteochondral repair presents a major challenge due to existing limitations and an urgent clinical need remains for an off-the-shelf, low cost, one-step approach. A biomimetic approach, where the biomaterial itself encourages cellular infiltration from the underlying bone marrow and provides physical and chemical cues to direct these cells to regenerate the damaged tissue, provides a potential solution. To meet this need, a multi-layer collagen-based osteochondral defect repair scaffold has been developed in our group. The objective of this study was to assess the *in vivo* response to this scaffold and determine its ability to facilitate differentiation of host stem cells in each layer in order to repair osteochondral tissue in a critical-sized defect in a rabbit knee. Multi-layer scaffolds were implanted into critical size (3 x 5mm) osteochondral defects created in the medial femoral condyle of the knee joint of New Zealand white rabbits and compared to an empty control group. Repair was assessed macroscopically, histologically and using micro-CT analysis at 12 weeks post implantation. Analysis of repair tissue demonstrated an enhanced macroscopic appearance in the multi-layer scaffold group compared to the empty group. In addition, diffuse host cellular infiltration in the scaffold group resulted in tissue regeneration with a zonal

organisation, with repair of the subchondral bone, formation of an overlying cartilaginous layer and evidence of an intermediate tidemark. These results demonstrate the potential of this biomimetic multi-layered scaffold to support and guide the host reparative response in the treatment of osteochondral defects.

Introduction

Cartilage has a limited capacity to regenerate following injury and thus poses a significant clinical problem. Osteochondral defects involving the smooth cartilage lining of the articulating surface and the underlying subchondral bone, are particularly problematic as they frequently occur in young active patients due to diseases such as osteochondritis dissecans, or as a result of traumatic injury to the joint. While some treatment options, such as microfracture, mosaicplasty and autologous chondrocyte implantation (ACI), are available to orthopaedic surgeons, success using these techniques is limited and frequently does not result in long lasting repair of the defect. This can eventually lead to the requirement for joint replacement. Cartilage is avascular and chondrocytes, the cellular components of cartilage, are present in low numbers and have poor mitotic ability. These inherent properties of cartilage tissue contribute significantly to its limited regenerative capacity. Regenerative medicine offers some promise in the area but the identification of a suitable cell source poses a significant challenge in the development of strategies for cartilage repair. Autologous chondrocytes, harvested and expanded prior to implantation into the site of damage, is one commonly used cell source. This approach has a number of associated limitations including, low numbers of suitable cells, *in vitro* de-differentiation, donor-site morbidity, the requirement for a two-step procedure, and high costs. Other potential cell sources are under investigation, including chondrocytes from non-articular sources and MSCs harvested from various locations including the bone marrow, adipose tissue and peripheral blood; however, their use clinically is still limited. An urgent clinical need thus remains for an off-the-shelf, low cost, one-step approach to chondral and osteochondral defect repair. In order to meet this need and overcome the requirement for an external cell source, there is now growing focus on the use of a biomaterials-based approach, where rather than supply cells to the defect site, the ideal biomaterial might encourage the

infiltration of cells from the underlying bone marrow and provide physical and biochemical cues to direct these cells to regenerate the damaged tissue [1,2,3].

A number of biomaterials-based approaches to osteochondral defect repair have emerged in recent years. However, such materials tend to consist of separate cartilage and bone repair scaffolds that are fused together using sutures or biological glues rather than truly addressing the integrated layered structure of osteochondral tissues. In addition, the research focus has been mainly on the chondral region of the defect site and has thus neglected the subchondral bone and calcified cartilage regions. It is now recognised that subchondral bone injury can play an important role in the development and progression of degenerative joint disease [4,5]. Thus regeneration of healthy subchondral bone within the defect site is essential in order to achieve completed repair within an osteochondral defect. The calcified cartilage and tidemark regions of the tissue also play a significant role by providing a stable interface between bone and cartilage and play a critical role in preventing vascular invasion from the subchondral bone into the chondral region which can lead to undesirable bony ingrowth. Until now however, no solution exists that addresses the complex challenge of repairing the cartilage, calcified cartilage and the underlying subchondral bone in osteochondral lesions. To meet this need, a biomimetic multi-layered collagen-based scaffold, has recently been designed and developed within our research group for the repair of osteochondral defects [6,7]. This biomimetic scaffold mimics the stratified composition of native osteochondral tissue by seamlessly integrating three distinct collagen-based layers using a novel iterative layering freeze-drying technique. The result is a multi-layered scaffold consisting of a base layer, previously optimised alone for bone repair [8,9], composed of type I collagen and hydroxyapatite (HA); an intermediate layer composed of type I and type II collagen and HA; and a superficial layer, previously optimised for cartilage repair, composed of type I and type II collagen in addition

to the glycosaminoglycan hyaluronic acid (HyA) (Fig. 1). This multi-layered scaffold, is characterised by seamless integration between layers, a high porosity with a highly interconnected pore structure [6]. The extracellular matrix macromolecules and biomechanical properties of this scaffold are designed to direct the differentiation of cells to produce cartilage, calcified cartilage and bone within each region of the scaffold. This scaffold has shown promising results *in vitro* and thus in order to assess its potential for translation into clinical use, assessment *in vivo* in an animal model is required.

The objective of this study was to assess the *in vivo* response of this biomimetic collagen-based multi-layered scaffold and determine its ability to facilitate the repair of osteochondral tissue in a critical-sized, weight bearing defect in a rabbit knee. The specific aims were to evaluate the scaffold's ability to support host cell infiltration and matrix deposition *in vivo*, and to investigate if the composition and micro-structure will direct cell differentiation within the distinct layers of the scaffold leading to tissue regeneration with a zonal organisation similar to that of native osteochondral tissue i.e. superficial articular cartilage, intermediate calcified cartilage and deep subchondral bone.

Materials and Methods

Multi-layered scaffold fabrication

Multi-layered collagen-based osteochondral scaffolds were fabricated as previously described [6]. Briefly, this involved fabrication of individual collagen-based suspensions for the bone layer, intermediate layer and cartilage layer of the scaffold. The bone layer contains 0.5% (w/v) microfibrillar bovine tendon type I collagen (Col1) (Collagen Matrix Inc., NJ, USA) and 1% (w/v) Hydroxyapatite (HA) powder (Captal 'R' Reactor Powder, Plasma Biotal, UK). The intermediate layer contains type I collagen (Col1), type II collagen (Col2) (Porcine type 2

collagen, Biom'up, Lyon, France) in 0.5 M acetic acid and adding HA to give final concentrations of 0.5% (w/v) Col1, 0.5% (w/v) Col2 and 0.2 % (w/v) HA. The cartilage layer consists of 0.125% (w/v) Col1, 0.375% (w/v) Col2 and 0.05% (w/v) HyA. A novel 'iterative layering freeze-drying' process was used to fabricate multi-layered scaffolds [6,7]. Briefly, 15.6 ml of the base layer suspension was pipetted into a stainless-steel tray (internal dimensions, 60 mm x 60 mm) before being freeze-dried (Virtis Genesis 25EL, Biopharma, Winchester, UK) at a constant cooling rate of 1°C min^{-1} to a final freezing temperature of -40°C [10,11]. Following freeze-drying, the base layer was cross-linked using 1-ethyl-3–3-dimethyl aminopropyl carbodiimide (EDAC)/N-hydroxysuccinimide (NHS) (Sigma–Aldrich, Arklow, Ireland) crosslinking at a ratio of 5:2 M and a 6 mM concentration of EDAC g^{-1} of collagen. The intermediate layer was formed by pipetting 7.8 ml of the intermediate layer suspension on top of the hydrated base layer scaffold and freeze-drying as before. Following rehydration, 15.6 ml of the cartilage layer suspension was pipetted on top of it and freeze-dried using prolonged freezing and drying steps. Following freeze-drying, the porous multi-layered scaffolds were dehydrothermally (DHT) cross-linked in a vacuum oven (VacuCell, MMM, Germany) for 24 hours at a pressure of 0.05 bar and a temperature of 105°C. Scaffolds were cut to 3.5 mm in diameter using a biopsy punch prior to surgery.

Osteochondral defect creation and multi-layered scaffold implantation in a rabbit knee

In vivo assessment was carried out in the rabbit medial femoral condyle model under ethical approval (Trinity College Dublin - Ref:191109) and an animal license granted by the Irish Government Department of Health (Ref: B100/4317). A total of eight skeletally mature (9 months old) female New Zealand White rabbits (Centre for Biomedical Science Education, Queens University Belfast, UK) of mean weight 3.2 kg (range 2.8-3.6 kg) were used in the study. Under anaesthetic, animals were positioned on their left side and an incision was made

using a medial parapatellar arthrotomy approach and lateral dislocation of the patella to gain access to the femoral condyle. A critical-sized defect, 3 mm diameter full-thickness osteochondral defect was created using a surgical drill (J.B. Tough Dental Ltd., Wicklow, Ireland) on the load-bearing area medial femoral condyle to a depth of 5 mm under constant irrigation (Fig. 2a). Animals were randomly assigned to the empty defect group (n=4) or the multi-layered scaffold group (n=4). In the empty defect group, the defects were left empty with no treatment applied. Defects in the multi-layered scaffold group were treated with a sterile cylindrical multi-layered scaffold press-fitted into the defect until level with the native cartilage surface (Fig. 2b). Scaffolds were hydrated in saline prior to implantation. Animals were housed in individual pens for 5 days post-surgery in order to restrict activity during the initial stages of healing and then transferred to group pens for the remainder of the study. Analgesia and antibiotics were administered for 5 days post-surgery (Carprofen 5mg/kg s/c and Enrofloxacin 10 mg/kg s/c pre- and post-surgery). Animals were euthanised at 12 weeks post implantation and the distal femur harvested for further analysis.

Macroscopic assessment

The macroscopic appearance of repair tissue in each operative site was blindly assessed by three individuals using the International Cartilage Repair Society (ICRS) cartilage repair assessment tool as shown in Table 1. This tool rates cartilage repair tissue as Grade IV (severely abnormal), Grade III (abnormal), Grade II (nearly normal) or Grade I (normal) based on the degree of defect repair, degree of integration and macroscopic appearance.

Microcomputed tomography

Microcomputed tomography (micro CT) was performed on all samples using a Scanco Medical 40 Micro CT system (Scanco Medical, Bassersdorf, Switzerland) with 70 kVP X-ray source

and 112 μA (resolution of ~12μm). Three-dimensional reconstructions were performed using a threshold of 140 in a scale from 0 – 1000. A volume of interest (VOI) was defined in order to assess healing within the subchondral bone region of the defect site. Repair was expressed as percentage bone volume over total volume (% BV/TV).

Histological analysis

Formalin fixed samples were decalcified using 15% ethylenediaminetetraacetic acid (EDTA, Fluka BioChemika, Sigma-Aldrich), bisected in the longitudinal axis using the lateral border of the intercondylar notch as a guide, and processed using an automated tissue processor (ASP300, Leica, Germany) before being embedded in paraffin wax blocks. Sections (7μm) were cut using a rotary microtome (Microsystems GmbH, Germany) and mounted on poly-L-lysine coated glass slides (Thermo Scientific, Menzel & Co KG, Germany). Sections were stained using Haematoxylin and Eosin (H&E) staining to examine repair tissue morphology, composition and arrangement, cell infiltration, extracellular matrix (ECM) production and scaffold degradation, Toluidine Blue and Safranin-O/Fast green staining, to assess the presence of proteoglycans and glycosaminoglycans and Masson's trichrome staining to identify collagen. Sections were examined microscopically using standard bright-field and polarised light microscopy and digital images captured (Nikon Microscope Eclipse 90i with NIS Elements software v3.06, Nikon Instruments Europe, The Netherlands).

Statistical analysis

Statistical differences between two treatments were assessed by student's paired t-test. Results are reported in figures as mean ± standard deviation and significance was determined using a probability value of $p<0.05$.

Results

Clinical observations and macroscopic evaluation

All animals recovered well post-surgery and within 3 days, ambulated freely with no signs of distress or limping for the duration of the study. On opening the joint 12 weeks post-surgery, there was evidence of glossy regenerated tissue similar to the surrounding host tissue in the multi-layered scaffold group (Fig. 3a). There was no evidence of an inflammatory reaction or degenerative change, construct delamination or loss into the joint cavity in the treated joints based on visual assessment at the time of retrieval. Fibrous and necrotic tissue was observed in the defect site of the empty defect group with cartilage-like tissue formation noted at the periphery in some cases; however this tissue showed a lack of continuity with native tissue. Macroscopic evaluation of the repair tissue was carried out using the ICRS cartilage repair assessment tool. Despite intragroup variability, the results showed that multi-layered scaffold treated animals had an average ICRS score of 8.9/12, placing them in the Grade II (nearly normal) category. In comparison, the empty defect group had a lower average ICRS score of 7.1/12 categorising them as a Grade III (abnormal) score (Fig. 3b). Noticeable depressions were observed in the central region of the defect site in the empty defect group. In contrast, improved integration with native tissue was seen in the multi-layered scaffold group with less obvious central depression and less fissuring of the surface.

Microcomputed tomography

The multi-layered scaffold group induced extensive bone repair within the subchondral region of operated knees by 12 weeks post-surgery. Qualitative evaluation of 2D projection images showed that multi-layered scaffold implanted knees showed advanced stages of bone repair (Fig. 4b). Bone formation in the multi-layered scaffold group appears to be adopting a structure similar to that of native bone with denser tissue near the surface adjacent to native cortical

bone, overlaying tissue with features of trabecular bone. This regenerated bone remained confined to the subchondral region of operated knees and did not extend above this level into the cartilage region. Quantification of bone formation in the multi-layered scaffold group was found to be significantly greater than that in the empty defect group (Fig. 4c).

Histological analysis

Histological analysis was consistent with micro-CT assessment with greater levels of bone formation observed within the defects treated with the multi-layered scaffold group compared to empty defect controls. Despite intragroup variability, major histological differences were demonstrated between multi-layered scaffold and empty defect groups. Adequate healing of the osteochondral defect was not seen in the empty defect group, with all empty defects noted to have deep fissuring, large residual void spaces, subchondral cyst formation, poor bone repair and mainly fibrous tissue formation (Fig. 5a and 6a). Notable findings in the multi-layered scaffold group were the regeneration of bone tissue within the subchondral region and the formation of an overlying cartilage layer (Fig. 5b and 6b). However, some areas of scaffold depression (Fig. 5b), shallow fissuring and areas of fibrocartilage were seen within the multi-layered scaffold group. Polarised light microscopy confirmed that the newly regenerated subchondral bone had already adopted a concentric lamellar pattern seen in mature subchondral trabecular bone by 12 weeks post-surgery (Fig. 6d). No regions of avascular necrosis were observed in the multi-layered scaffold group, although one sample was found to contain a small subchondral cyst (Fig. 5b).

Cells and matrix were present in all samples in the multi-layered scaffold group indicating that host cells had successfully infiltrated throughout the scaffold post-implantation. By 12 weeks these cells exhibited distinct morphologies depending on their location, gradually transitioning

from superficial chondrocytes to osteocytes in the deep subchondral bone (Fig. 7a). Furthermore, the presence of an intermediate basophilic tidemark (TM) was also observed between the regenerated cartilage and bone (Fig. 7a). This tidemark signified the limiting line for calcification and vascularisation with no areas of bone or blood vessel formation seen in the cartilage region above this line. Below the tidemark areas with similar appearances to native bone, including neovascularsation were seen (BV) (Fig. 7a). There was continuity between the different regions of regenerate tissue indicating that scaffolds had maintained their internal integrity and resisted interfacial delamination *in vivo*.

Cells in the superficial region, particularly those located towards the periphery of the implantation site, displayed a rounded morphology and were found residing within lacunae (Fig. 7a and 7b), characteristics typical of chondrocytes in native cartilage. Furthermore, a cellular alignment typical of cartilage and matrix positive for glycosaminoglycans was also seen in relation to these cells (Fig. 7b). In the intermediate region, collagen fibres at the junction of newly formed cartilage and bone tissue displayed a vertical orientation on polarized light (Fig. 7c). This is similar to that normally seen at the calcified cartilage region intervening between subchondral bone and articular cartilage in osteochondral tissue. Furthermore, this region coincided with the basophilic tidemark (Fig. 7c).

Extensive scaffold replacement was noted with most of the original scaffold material no longer visible. Only small remnants of scaffold were observed within the defect site of one animal (Fig. 7d). The newly formed bone had fully integrated with the surrounding host bone and the original defect boundary was not visible after 12 weeks *in vivo*. Osteon development with Haversian canals, osteocytes and mature lamellar bone was seen embedded within the

regenerated matrix of the subchondral region previously occupied by the scaffold base layer (Fig. 7e and 7f).

Discussion

Despite numerous advances in the treatment of damage to the articular cartilage, an urgent unmet clinical need remains for an off-the-shelf, low cost, one-step approach to osteochondral defect repair. In order to address this need, a biomimetic multi-layered collagen-based scaffold has been designed within our group for osteochondral defect repair. This highly porous scaffold has previously demonstrated biocompatibility and the potential for cells to attach to and infiltrate through its porous microstructure [6]. The overall aim of this study was to assess the *in vivo* response of this multi-layered scaffold and determine its potential to facilitate the repair of osteochondral tissue in a critical-sized, weight bearing defect in a rabbit knee. Specifically, we investigated the scaffold's ability to support host cellular infiltration and matrix deposition *in vivo* and investigated if the layered arrangement of the scaffold led to tissue regeneration with a zonal organisation similar to that of native osteochondral tissue. Results showed that the scaffold enhanced the macroscopic appearance of the articular surface, as assessed using an ICRS evaluation tool, compared to empty defect controls. Histological analysis showed diffuse cellular infiltration and matrix production throughout the scaffold 12 weeks post-surgery. Staining revealed cartilaginous tissue in the superficial region of the defect site overlying significant new subchondral bone formation, confirmed by micro CT evaluation. Furthermore, a calcified cartilage-like layer was observed between the bone and cartilage layers and was associated with a newly formed tidemark.

The multi-layered scaffold facilitated host cell infiltration resulting in construct cellularisation, neotissue formation and enhanced healing. The highly porous and highly interconnected pore

303 structure of the multi-layered scaffold has previously been shown to support cellular infiltration
304 and proliferation *in vitro* [6] and the results reported here demonstrate its ability to permit host
305 cell infiltration *in vivo*. The scaffold rapidly absorbed blood and bone marrow immediately
306 post-implantation as evidenced by the change in colour of the scaffold from white to red (Fig.
307 2b). Histological assessment showed that host cells were able to homogeneously distribute
308 throughout the scaffold. This thus confers a major advantage over cell-based repair techniques
309 that require at least two surgeries with prolonged intervening *in vitro* cultivation periods to
310 ensure cellularisation prior to implantation [12]. Therefore, the multi-layered scaffold
311 investigated herein, might allow for a one-step operative approach, reducing both the surgical
312 and economic burden [13]. Additionally, this scaffold relies purely on its composition and
313 biostructural and biomechanical properties to achieve this response thus negating the
314 requirement for additional biomolecules that have shown some success in other recent
315 investigations [14,15,16,17].
316
317 Macroscopic differences evident in the superficial cartilage region of the defects indicated the
318 benefit of the multi-layered scaffold in promoting cartilage regeneration *in vivo*. Blinded
319 macroscopic assessment of retrieved samples revealed that the multi-layered scaffold group
320 had a Grade II (8.9/12) score (nearly normal) using the ICRS cartilage repair assessment tool
321 (Fig. 3b). It has recently been used in the assessment of cartilage repair techniques used to treat
322 cartilage defects in young competitive athletes which demonstrated that higher scores were
323 consistent with return to preoperative activity including competitive sport [18,19]. The
324 presence of surface depression and fissuring of repair tissue were observed and may be relate
325 to pressure from synovial fluid within the joint. Furthermore, one sample was found to have
326 developed a small subchondral cyst, similar to findings previously reported and attributed to
327 such synovial fluid pressures [20,21,22].

Histological evaluation showed that infiltrating cells appeared to adopt region specific morphologies including characteristics typical of chondrocytes (Fig. 7a and 7b) and osteocytes (Fig. 7e) in cartilage and bone regions respectively. Following implantation, host cells were absorbed into this hydrophilic collagen-based scaffold and adhered to individual struts within the different scaffold layers. The layer-specific mechanical and compositional properties of these struts likely played a role in guiding host cell differentiation towards a chondrogenic lineage in the type II collagen-hyaluronic acid superficial layer or an osteogenic lineage in the collagen-HA base layer, thus allowing independent but simultaneous tissue formation in each region. It is recognised that the mechanical properties [23,24,25] and composition [26,27,28,29,30,31,32] of a substrate can affect cell differentiation *in vitro*. Specifically, the chondrogenic properties of type II collagen and hyaluronic acid have previously been demonstrated [26,27,28] and the addition of hydroxyapatite to highly porous collagen-based scaffold has been shown to improve their osteogenic [29,30] and osteoinductive properties [31,32]. Given that differences in compressive modulus have previously been observed between the layers of this scaffold[6], it is likely that these differences influenced host cell response and tissue formation following *in vivo* implantation. Furthermore, quantitative assessment demonstrated the potential of this scaffold to promote a significantly higher level of bone formation *in vivo* compared to controls (Fig. 4) and showed that the regenerated bone remained confined to the subchondral region.

The inclusion of a calcified cartilage region within the multi-layered scaffold and the formation of a tidemark prevented the migration of subchondral bone and vasculature towards the joint surface. The natural boundary between vascularised subchondral bone and avascular articular cartilage at the chondro-osseous junction is the tidemark, found on the superior aspect of the

calcified cartilage layer [33]. Upward migration of subchondral bone has been reported in between 25-34% of patients post-ACI [34,35] and *in vivo* assessments of grafts for osteochondral lesion repair have previously failed to spatially restrict bone and vessel growth to the subchondral region following intra-articular implantation [36]. In such an event, direct bone-on-cartilage contact between an ossified graft and the opposing host articular surface within a dynamic joint could cause chondral damage and early progression towards degenerative change [37]. Several interventions have attempted to prevent bone and vessel overgrowth by employing physical or chemical barriers to compartmentalise tissue formation and prevent bone growth in the superficial zone [38,39]. However, in this current study the inclusion of a calcified cartilage region within the multi-layered scaffold and the formation of a tidemark, (Fig. 7a), signified the limiting line for calcification and vascularisation. This is very encouraging and resulted in bone and vessel formation being restricted to the subchondral region (Fig. 7c), thus maintaining an unmineralised avascular cartilage layer.

The press-fit implantation method used enabled the scaffold to be maintained securely within the defect site allowing for its degradation and replacement with newly formed bone and cartilage. Previous studies have observed difficulties with achieving integration between implants and native tissue [40,41] and in achieving a balance between scaffold degradation and tissue formation [42]. Other natural polymer scaffolds for osteochondral repair have failed to adequately degrade and integrate with host tissues resulting in poor defect healing [37]. Therefore, the biomimetic composition of the multi-layered scaffold may have facilitated enhanced integration at interface regions between the neotissue formed and host tissue. Histological analysis also demonstrated that apart from small remnants of one scaffold, all scaffolds had been replaced with nascent bone and cartilage tissue (Fig. 7d). Additionally, the seamless integration of layers within the multi-layered scaffold was maintained *in vivo*.

Layered scaffolds have previously been fabricated from individual layers that were subsequently bonded together using agents such as fibrin glue [43,44].This approach presents potential disadvantages as the bonding agents may inhibit cellular infiltration between layers [45].The iterative fabrication process used here achieves strong adherence between layers that has been shown to maintain layer interconnectivity during mechanical testing *in vitro* [6]. Furthermore, the *in vivo* assessment carried out in this study suggests its ability to maintain its continuity during unrestricted joint movement over the experimental period.

Overall, this study demonstrates the *in vivo* proof of concept and significant promise of utilising this multi-layered scaffold for osteochondral defect repair. The rabbit model used is a recommended model for preliminary investigations of devices designed for cartilage/osteochondral repair [46,47,48] and is the most commonly used model for the evaluation of multilayer scaffolds for osteochondral repair [3]. However, in order to further assess the regenerative capacity of the multi-layered scaffold, *in vivo* analysis in larger animal models (caprine and equine) with joints that more closely represent those of humans, is required. While this study has some recognised limitations including small numbers and intragroup variability, the results successfully demonstrate the ability of this biomimetic multi-layered scaffold to support and guide the host reparative response. This approach, when followed by the use of larger animal models, allows for step-wise progression towards translation of new biomaterials to the clinic.

Conclusions

In conclusion, this study demonstrates the successful *in vivo* application of a collagen-based multi-layered osteochondral defect repair scaffold in a critical-sized defect in a rabbit knee.

The scaffold extracellular matrix macromolecules and biomechanical properties are designed to provide an ideal environment for cell attachment and proliferation and to direct the differentiation of cells to produce cartilage, calcified cartilage and bone within each region of the scaffold. Greater levels of repair were observed in the multi-layer scaffold group compared to the empty group at 12 weeks post implantation. The results demonstrate that diffuse host cellular infiltration in the multi-layered scaffold group resulted in tissue regeneration with a zonal organisation, with repair of the subchondral bone, formation of an overlying cartilaginous layer and evidence of an intermediate tidemark. Overall, these results show the potential of this biomimetic multi-layered scaffold to support and guide the host reparative response in the treatment of osteochondral defects.

Acknowledgements

The authors acknowledge Enterprise Ireland Proof of Concept Award (PC/2007/331) and Commercialisation Fund Technology Development Award (CFTD/2009/0104) and Science Foundation Ireland (SFI)/ Health Research Board (HRB) Translational Research Award (TRA/2011/19) for funding.

Conflict of Interest

Authors John P Gleeson and Fergal J O'Brien hold IP with a commercial product of related composition to the collagen-based scaffolds used in this study.

References

1. M. Keeney, A. Pandit. The osteochondral junction and its repair via bi-phasic tissue engineering scaffolds. Tissue Eng Part B. 15 (2009) 55-73.

426 2. S.P. Nukavarapu, D.L. Dorcemus. Osteochondral tissue engineering: current strategies and
427 challenges. Biotechnol Adv. 31(2013) 706-21.

428 3. J.E. Jeon, C. Vaquette, T.J. Klein, D.W. Hutmacher. Perspectives in multiphasic
429 osteochondral tissue engineering. Anat Rec. 297 (2014) 26-35.

430 4. A. Lahm, P.C. Kreuz, M. Oberst, J. Haberstroh, M. Uhl,. D. Maier. Subchondral and
431 trabecular bone remodeling in canine experimental osteoarthritis. Arch Orthop Trauma Surg.
432 126 (2006) 582-7.

433 5. E.H. Mrosek, A. Lahm, C. Erggelet, M. Uhl, H. Kurz, B. Eissner, J.C. Schagemann.
434 Subchondral bone trauma causes cartilage matrix degeneration: an immunohistochemical
435 analysis in a canine model. Osteoarthr Cartilage. 14 (2006) 171-8.

436 6. T.J. Levingstone, A. Matsiko, G.R. Dickson, F.J. O'Brien, J.P. Gleeson. A biomimetic multi-
437 layered collagen-based scaffold for osteochondral repair. Acta Biomater. 10(5) (2014) 1996-
438 2004.

439 7. J.P. Gleeson, T.J. Levingstone, F.J. O'Brien. Layered scaffold suitable for osteochondral
440 defect repair. Patent WO2010/084481, 2009.

441 8. J.P. Gleeson, N.A. Plunkett, F.J. O'Brien. Addition of hydroxyapatite improves stiffness,
442 interconnectivity and osteogenic potential of a highly porous collagen-based scaffold for bone
443 tissue regeneration. Eur Cell Mater. 20 (2010) 218-30.

444 9. F.G. Lyons, J.P. Gleeson, S. Partap, K. Coghlan, F.J. O'Brien. Novel microhydroxyapatite
445 particles in a collagen scaffold: a bioactive bone void filler? Clin Orthop Relat R. 472(4) (2014)
446 1318-1328

447 10. F.J. O'Brien, B.A.Harley, I.V. Yannas, L.J. Gibson. Influence of freezing rate on pore
448 structure in freeze-dried collagen-GAG scaffolds. Biomaterials. 25 (2004) 1077-86.

449 11. F.J. O'Brien, B.A. Harley, I.V. Yannas, L.J. Gibson. The effect of pore size on cell adhesion
450 in collagen-GAG scaffolds. Biomaterials. 26 (2005) 433-41.

451 12. M. Brittberg. Cell Carriers as the Next Generation of Cell Therapy for Cartilage Repair A
452 Review of the Matrix-Induced Autologous Chondrocyte Implantation Procedure. Am. J. Sports
453 Med. 38 (2010) 259-1271.

454 13. E. Kon, G. Filardo, B. Di Matteo, F. Perdisa, M. Marcacci. Matrix assisted autologous
455 chondrocyte transplantation for cartilage treatment: A systematic review. Bone Joint Res. 2
456 (2013) 18-25.

457 14. H. Maehara, S. Sotome, T. Yoshii, I. Torigoe, Y. Kawasaki, Y. Sugata, M. Yuasa, M.
458 Hirano, N. Mochizuki, M. Kikuchi, K. Shinomiya, A. Okawa.. Repair of large osteochondral
459 defects in rabbits using porous hydroxyapatite/collagen (HAp/Col) and fibroblast growth
460 factor-2 (FGF-2). J Orthop Res. 28 (2010) 677-686.

461 15. N. Mohan, N.H. Dormer., K.L. Caldwell, V.H. Key, C.J. Berkland, M.S. Detamore.
462 Continuous gradients of material composition and growth factors for effective regeneration of
463 the osteochondral interface. Tissue Eng Part A.17 (2011) 2845-55.

464 16. R. Reyes, A. Delgado, E. Sanchez, A. Fernandez, A. Hernandez, C. Evora. Repair of an
465 osteochondral defect by sustained delivery of BMP-2 or TGF-beta1 from a bilayered alginate-
466 PLGA scaffold. J Tissue Eng Regen Med. 6 (7) (2014) 521-33.

467 17. T. Re'em, F. Witte, E. Willbold, E. Ruvinov, S. Cohen. Simultaneous regeneration of
468 articular cartilage and subchondral bone induced by spatially presented TGF-beta and BMP-4
469 in a bilayer affinity binding system. Acta Biomater. 8 (2012) 3283-3293.

470 18. R. Gudas, A. Gudaite, A. Pocius, A. Gudiene, E. Cekanauskas, E. Monastyreckiene A.
471 Basevicius . Ten-year follow-up of a prospective, randomized clinical study of mosaic

472 osteochondral autologous transplantation versus microfracture for the treatment of
473 osteochondral defects in the knee joint of athletes. Am J Sports Med. 40 (2012) 2499-508.

474 19. G. Panics., L.R. Hangody, E. Baló, G. Vásárhelyi, T. Gál, L. Hangody. Osteochondral
475 autograft and mosaicplasty in the football (soccer) athlete. Cartilage. 3 (2012) 25s-30s.

476 20. A. Getgood, F. Henson, C. Skelton, E. Herrera, R. Brooks, L.A. Fortier, N. Rushton.. The
477 augmentation of a collagen/glycosaminoglycan biphasic osteochondral scaffold with platelet-
478 rich plasma and concentrated bone marrow aspirate for osteochondral defect repair in sheep:
479 A pilot study. Cartilage. 3 (2012) 351-363.

480 21. A. Getgood, S.J. Kew, R. Brooks, H. Aberman, T. Simon, A.K. Lynn, N. Rushton. .
481 Evaluation of early-stage osteochondral defect repair using a biphasic scaffold based on a
482 collagen-glycosaminoglycan biopolymer in a caprine model. Knee, 19 (2012) 422-430.

483 22. F. Benazzo, M. Cadossi, F. Cavani, M. Fini, G. Giavaresi, S. Setti, R. Cadossi, R. Giardino.
484 Cartilage repair with osteochondral autografts in sheep: Effect of biophysical stimulation with
485 pulsed electromagnetic fields. J Orthop Res. 26 (2008) 631-642.

486 23. D.E. Discher, P. Janmey, Y.L. Wang. Tissue cells feel and respond to the stiffness of their
487 substrate. Science. 310 (2005) 1139–1143

488 24. D. Karamichos , R.A. Brown, V. Mudera. Complex dependence of substrate stiffness and
489 serum concentration on cell-force generation. J Biomed Mater Res. A78 (2) (2006) 407-15.

490 25. J.R. Tse and A.J. Engler. Stiffness gradients mimicking *in vivo* tissue variation regulate
491 mesenchymal stem cell fate, PLoS One. 6 (1) (2011) e15978.

492 26. A. Matsiko , T.J. Levingstone, F.J. O'Brien, J.P. Gleeson. Addition of hyaluronic acid
493 improves cellular infiltration and promotes early-stage chondrogenesis in a collagen-based
494 scaffold for cartilage tissue engineering J Mech Behav Biomed Mater. 11 (2012) 41-52.

27. G. Ragetly, D.J. Griffon, Y.S. Chung. The effect of type II collagen coating of chitosan fibrous scaffolds on mesenchymal stem cell adhesion and chondrogenesis. Acta Biomater. 6 (10) (2010) 3988–97.

28. K.Y. Chang, L.H. Hung, I.M. Chu, C.S. Ko, Y.D. Lee. The application of type II collagen and chondroitin sulfate grafted PCL porous scaffold in cartilage tissue engineering. J Biomed Mater Res A. 92 (2010) 712–723.

29. J.P. Gleeson, N.A. Plunkett, F.J. O'Brien. Addition of hydroxyapatite improves stiffness, interconnectivity and osteogenic potential of a highly porous collagen-based scaffold for bone tissue regeneration. Eur Cell Mater. 20 (2010) 218–230.

30. J.B. Vines, D.J. Lim, J.M. Anderson, H.W. Jun. Hydroxyapatite nanoparticle reinforced peptide amphiphile nanomatrix enhances the osteogenic differentiation of mesenchymal stem cells by compositional ratios. Acta Biomater. 8 (2012) 4053–4063.

31. H. Yuan, J.D. De Bruijn, X. Zhang, C.A. Van Blitterswijk, K. De Groot. Use of an osteoinductive biomaterial as a bone morphogenetic protein carrier. J Mater Sci Mater Med. 12 (2001)761–766.

32. C.M. Murphy, A. Schindeler, J.P. Gleeson, N.Y.C. Yu, L.C. Cantrill, K. Mikulec, L. Peacock , F.J. O'Brien, D.G. Little . A collagen–hydroxyapatite scaffold allows for binding and co-delivery of recombinant bone morphogenetic proteins and bisphosphonates. Acta Biomater. 10 (5) (2014) 2250-8.

33. F. Wang, Z. Ying, X. Duan, H. Tan, B. Yang, L. Guo, G. Chen, G. Dai, Z. Ma, L. Yang. Histomorphometric analysis of adult articular calcified cartilage zone. J Struct Biol. 168 (2009) 359-65.

517 34. I.J.P. Henderson, D.P. La Valette. Subchondral bone overgrowth in the presence of full-
518 thickness cartilage defects in the knee. Knee. 12 (2005) 435-440.

519 35. T. Minas, A.H. Gomoll, R. Rosenberger, R.O. Royce, T. Bryant. Increased Failure Rate of
520 Autologous Chondrocyte Implantation After Previous Treatment With Marrow Stimulation
521 Techniques. American Journal of Sports Medicine. 37 (2009) 902-908.

522 36. J.M. Coburn, M. Gibson, S. Monagle, Z. Patterson, J.H. Elisseeff. Bioinspired nanofibers
523 support chondrogenesis for articular cartilage repair. Proc Natl Acad Sci. 109 (2012) 10012-7.

524 37. A. Abarrategi, Y. Lopiz-Morales, V. Ramos, A. Civantos, L. Lopez-Duran, F. Marco, J.L.
525 Lopez Lacomba. Chitosan scaffolds for osteochondral tissue regeneration. J Biomed Mater Res
526 A. 95 (2010) 1132-41.

527 38. E.B. Hunziker, I.M. Driesang, C. Saager. Structural barrier principle for growth factor-
528 based articular cartilage repair. Clin Orthop Relat Res. (2001) S182-9.

529 39. E.B. Hunziker, I.M. Driesang. Functional barrier principle for growth-factor-based articular
530 cartilage repair. Osteoarthritis Cartilage. 11 (2003) 320-7.

531 40. D. Schaefer, I. Martin, G. Jundt, J. Seidel, M. Heberer, A. Grodzinsky, I. Bergin, G.Vunjak-
532 Novakovic, L.E. Freed . Tissue-engineered composites for the repair of large osteochondral
533 defects. Arthritis Rheum. 46 (2002) 2524-34.

534 41. C.H. Chang, T.F. Kuo, C.C. Lin, C.H. Chou, K.H. Chen, F.H. Lin, H.C. Liu. Tissue
535 engineering-based cartilage repair with allogenous chondrocytes and gelatin-chondroitin-
536 hyaluronan tri-copolymer scaffold: A porcine model assessed at 18, 24, and 36 weeks.
537 Biomaterials. 27 (2006) 1876-1888.

538 42. D.W. Hutmacher. Scaffolds in tissue engineering bone and cartilage. Biomaterials. 21
539 (2000) 2529-43.

43. C. Scotti, D. Wirz, F. Wolf, D.J. Schaefer, V. Burgin, A.U. Daniels, V. Valderrabano, C. Candrian, M. Jakob, I. Martin, A. Barbero. Engineering human cell-based, functionally integrated osteochondral grafts by biological bonding of engineered cartilage tissues to bony scaffolds. Biomaterials. 31 (2010) 2252-9.

44. J. Chen, H. Chen, P. Li, H. Diao, S. Zhu, l. Dong, R. Wang, T. Guo, J. Zhao, J. Zhang. Simultaneous regeneration of articular cartilage and subchondral bone *in vivo* using MSCs induced by a spatially controlled gene delivery system in bilayered integrated scaffolds. Biomaterials. 32 (2011) 4793-805.

45. B.A. Harley, A.K. Lynn, Z. Wissner-Gross, W. Bonfield, I.V. Yannas, L.J. Gibson. Design of a multiphase osteochondral scaffold III: Fabrication of layered scaffolds with continuous interfaces. J Biomed Mater Res A. 92 (2010) 1078-93.

46. ASTM. Standard Guide for *in vivo* Assessment of implantable devices intended to repair or regenerate articular cartilage. American Society for Testing and Materials, 2010.

47. C.R. Chu, M. Szczodry, S. Bruno. Animal models for cartilage regeneration and repair. Tissue Eng Part B Rev. 16 (2010) 105-15.

48. J.L. Cook, C.T. Hung, K. Kuroki, A.M. Stoker, C.R. Cook, F.M. Pfeiffer, S. L. Sherman, J. P. Stannard. Animal models of cartilage repair. Bone Joint Res. 3 (2014) 89-94.

Figures

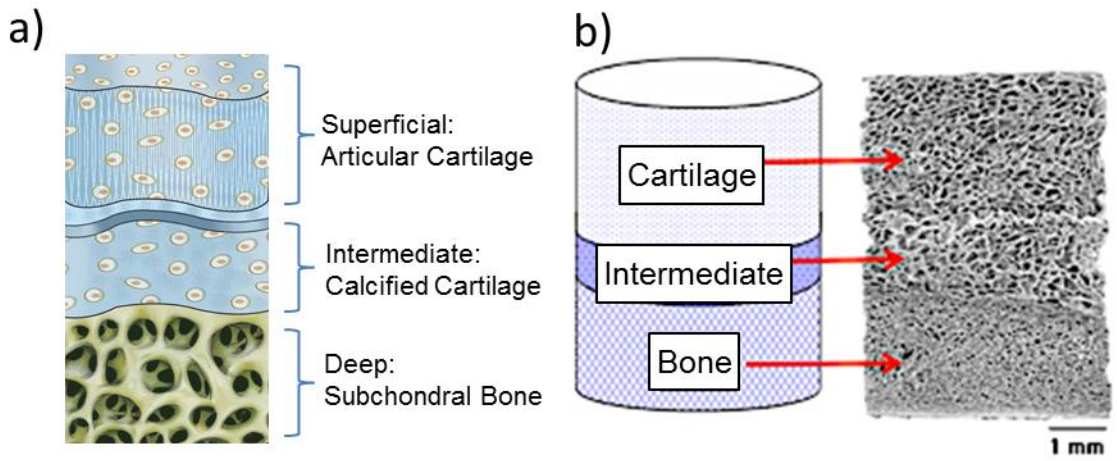

558

559 **Figure 1:** Schematic diagrams showing (a) the superficial, intermediate and deep layers of the
560 osteochondral region and (b) the multi-layered scaffold. This scaffold is fabricated using three
561 distinct collagen-based slurries sequentially freeze-dried to produce a highly porous,
562 seamlessly integrated multi-layered scaffold, as demonstrated by scanning electron microscopy
563 (extreme right), designed to mimic the composition and microstructural properties of the
564 osteochondral region.

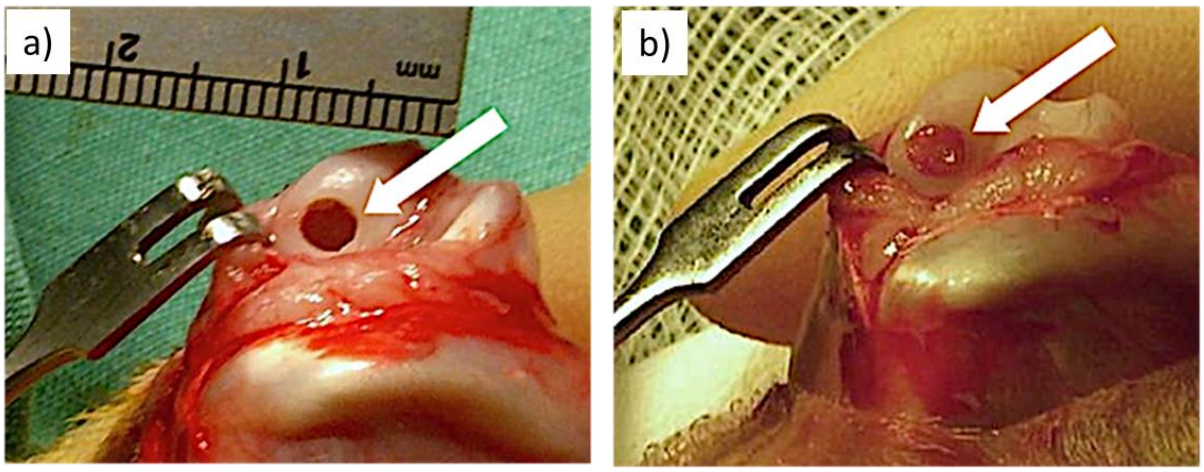

565

566 **Figure 2:** Multi-layered scaffolds were implanted into osteochondral defects (3 mm diameter
567 x 5mm depth) created on medial femoral condyle. Intraoperative photographs show a) the size
568 and location of the defect and b) Press-fit implantation of the multi-layered scaffold showing
569 the close-fitting relationship between the implant and surrounding tissue.

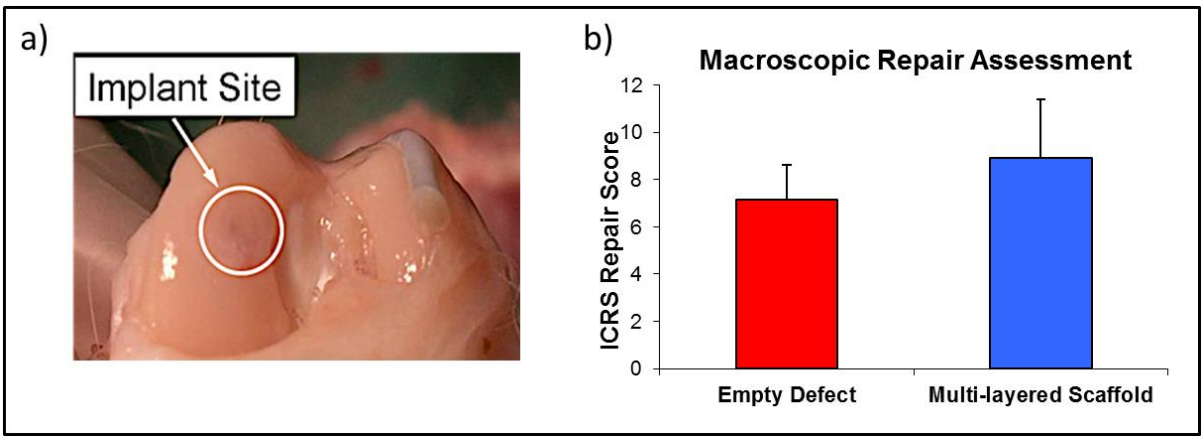

570

571 **Figure 3:** Improved macroscopic repair was observed in the multi-layer scaffold group
572 compared to the empty defect group at 12 weeks post implantation a) photograph showing
573 macroscopic appearance of the distal femur at 12 weeks post-surgery with neotissue
574 highlighted by the white circle b) Blinded quantitative macroscopic evaluation of repair tissue
575 formed in the empty defect and multi-layered scaffold groups by three investigators showed
576 that the multi-layered scaffold treated group had a higher average ICRS score compared to
577 controls. The values are expressed as mean ± standard deviation, n=4

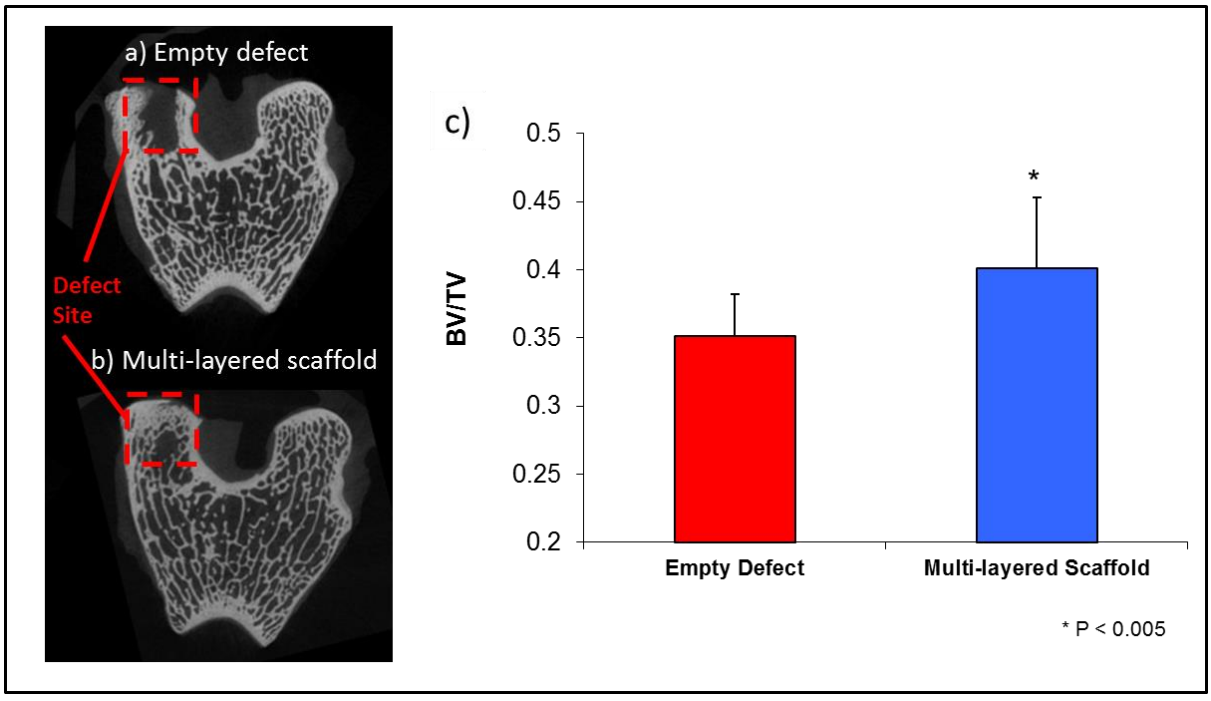

578

Figure 4: Micro-CT analysis at 12 weeks post-surgery showed greater levels of bone repair in the multi-layered scaffold group than the empty defect group. 2D projection images show the failure of subchondral bone restoration in the empty defect group (a). In comparison, the multi-layered scaffold group (b) showed enhanced repair of subchondral bone after 12 weeks. Quantitative micro-CT analysis of regenerated bone within the defect space of operated knees demonstrates significantly greater level of bone formation in the multi-layered scaffold group compared to the control group after 12 weeks in vivo (c). The values are expressed as mean ± standard deviation, n=4, *represents $p<0.05$ statistical significant differences relative to control group.

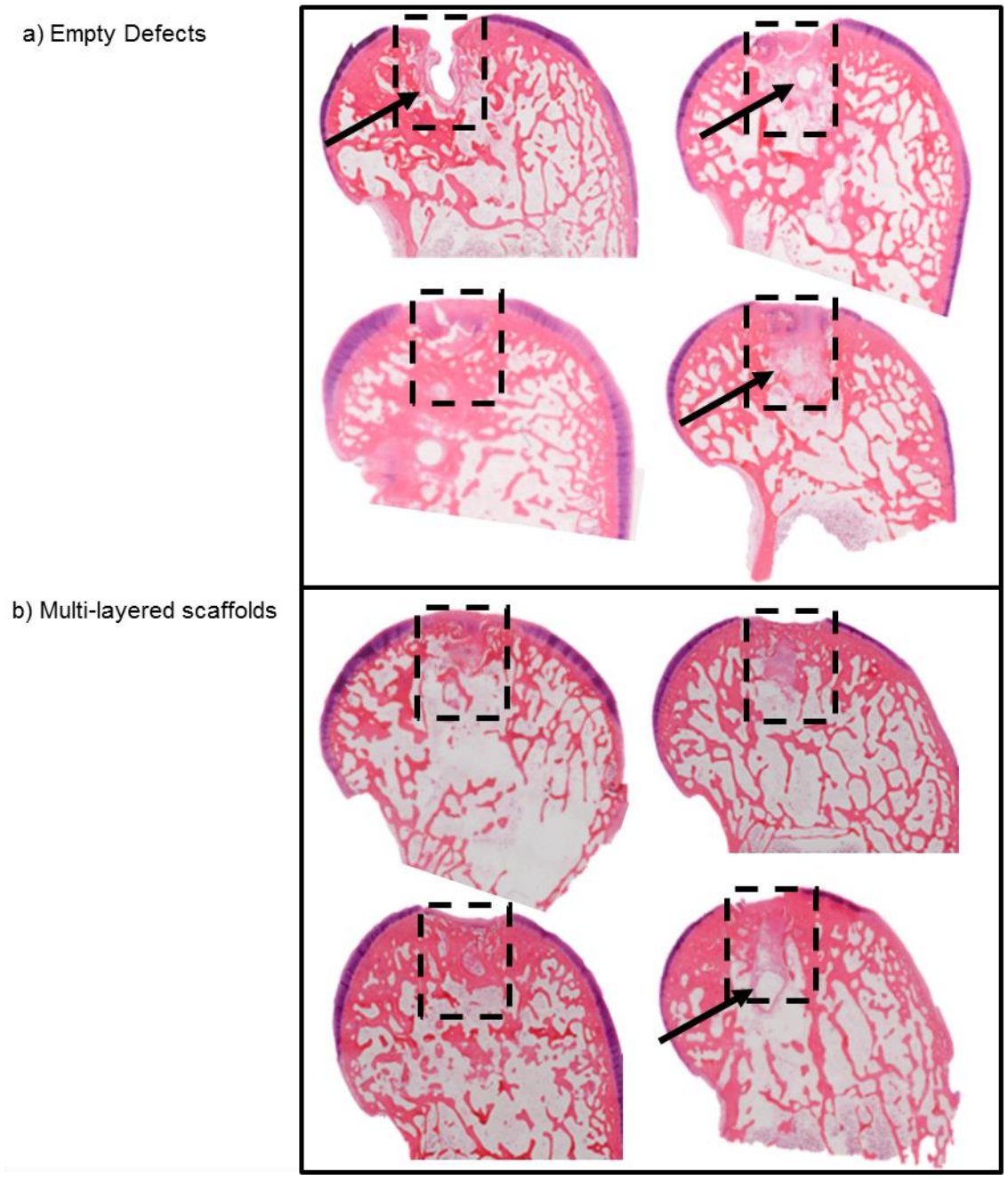

588

589 **Figure 5:** H&E stained representative images from each animal show the region of the defect
590 site and neotissue formed after 12 weeks in situ, highlighted with dashed lines. Slight
591 depression of the superficial surface was noted in both groups with subchondral cysts occurring
592 predominantly in the empty defect group (arrows).

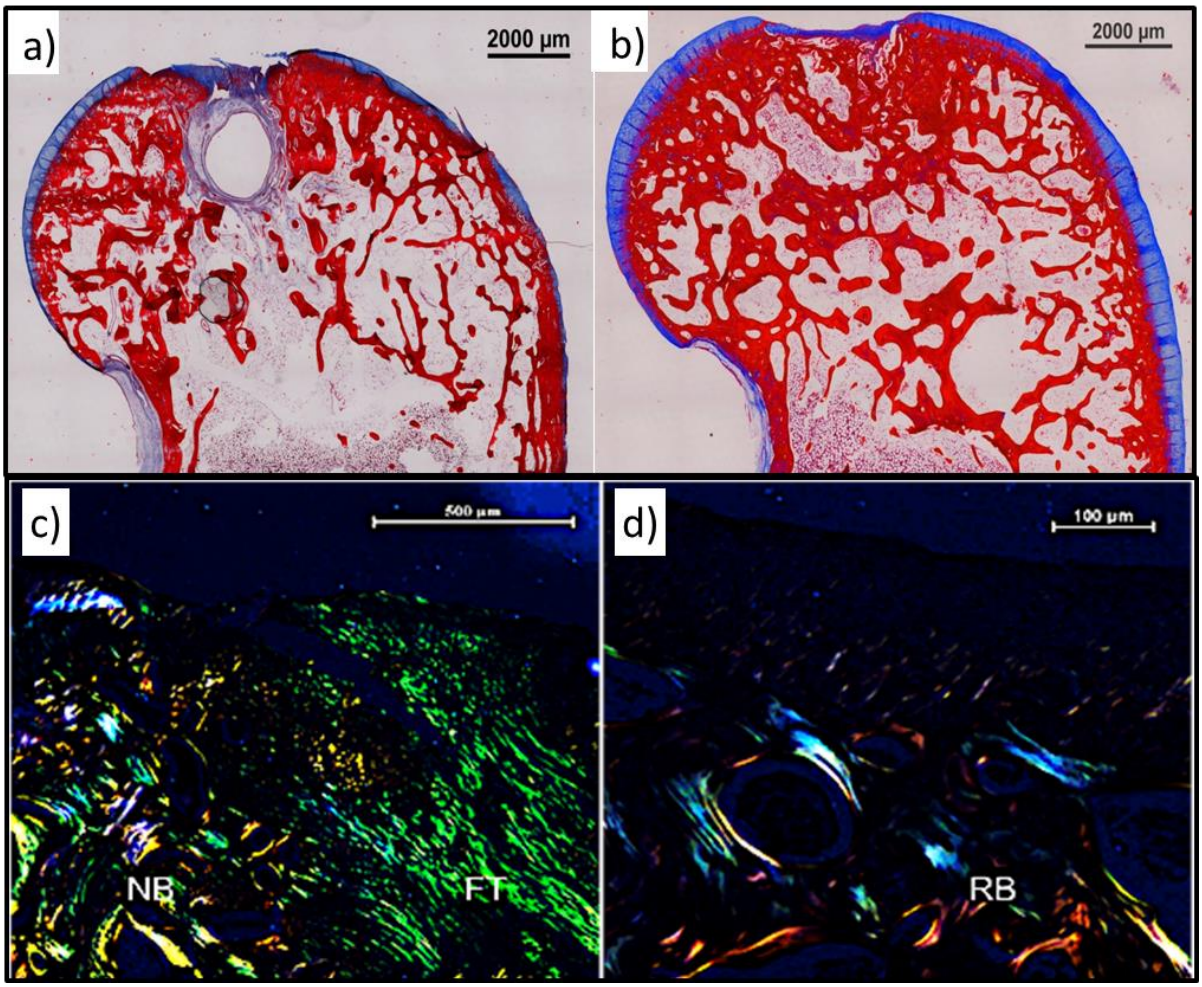

Figure 6: Masson's Trichrome stained images showing neo-tissue formation using bright-field (a,b) and polarised light (c,d,), in the empty defect (a,c) and multi-layered scaffold (b,d) groups at 12 weeks post-surgery –cartilage staining blue and bone staining red. Fibrous tissue with large residual void spaces within the subchondral bone region can be seen in the empty defect group (a). Multi-layered scaffolds displayed more advanced healing with regeneration of bone tissue within the subchondral bone and the formation of an overlying cartilage layer (b). Using polarised light microscopy, Fibrous tissue (FT) formation is seen in the empty defects (c) abutting native bone (NB). In contrast, multi-layered scaffolds (d) display regenerative bone (RB) adopting a concentric lamellar pattern of native subchondral bone.

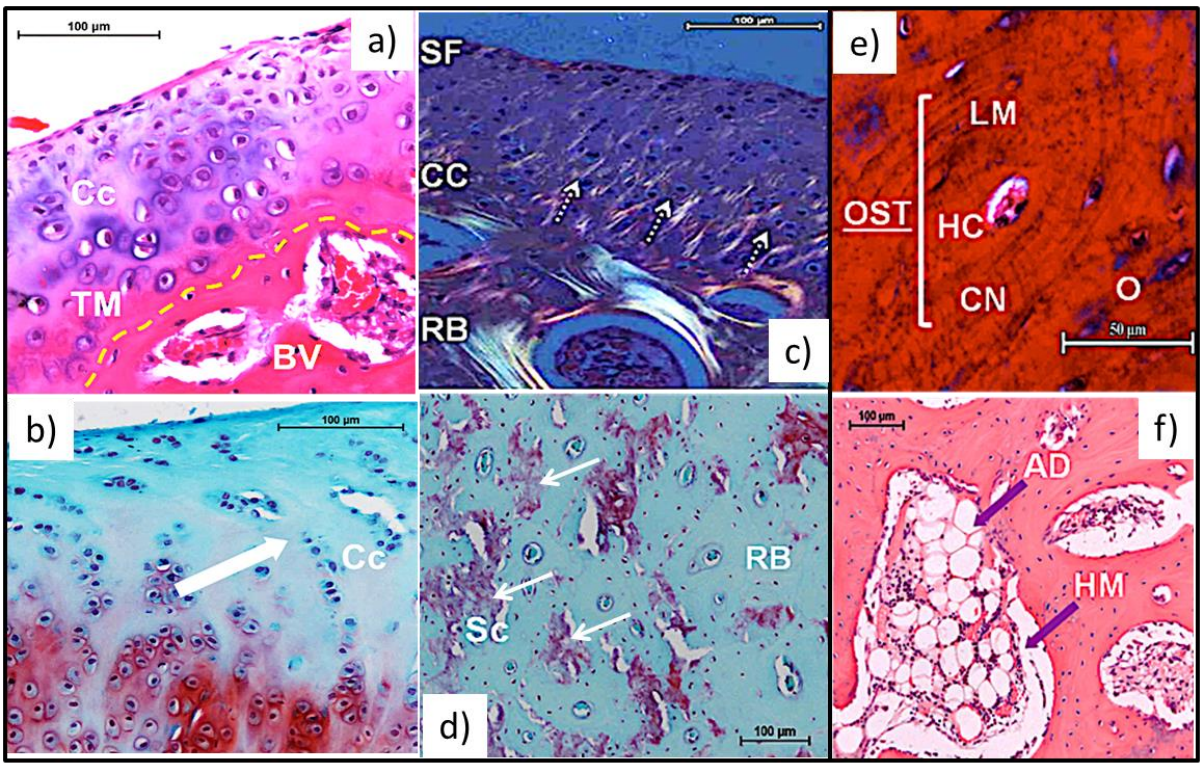

Figure 7: Histological analysis showed the formation of bone and cartilage within the defect site in the multi-layered scaffold group a) H&E stained histological image showing distinct cellular morphologies depending on location, transitioning from chondrocytes (Cc) to neovascularised subchondral bone (BV) with an intermediate basophilic tidemark (TM, highlighted in yellow). b) Safranin-O/fast green histological image showing cells (Cc) have adopted a hyaline-like cartilage arrangement with the production of sulphated glycosaminoglycans, staining red. c) Polarised light microscopy demonstrating the vertically orientation (white arrows) of collagen fibers in the transitional zone (CC) between superficial cartilage (SF) and regenerated bone (RB). d) H&E and Safranin-O/fast green image showing the presence of neo-tissue and some scaffold remnant (Sc: purple colour, highlighted with arrows) within the bone region with evidence of mature regenerated bone (RB: green) replacing the implanted scaffold. Qualitative Masson's trichrome (e) and H&E (f) histological image showing mature bone formation (e) with osteon (OST) formation including the presence of Haversian canals (HC), canaliculi (CN), osteocytes (O) and a lamellar bone pattern (LM) and

(f) restoration of the bone marrow cavity with highly cellularised regions resembling bone marrow containing hemopoietic cells (HM) and adipocytes (AD) were seen between bony trabeculae in the regenerated tissue adjacent to the host medullary cavity.

Table 1: International Cartilage Repair Society (ICRS) cartilage repair assessment tool. This tool is used by surgeons to evaluate the macroscopic appearance of cartilage repair tissue following interventions such as ACI, subchondral drilling and microfracture.

	Criteria	Points
Degree of Defect Repair	Level with surrounding cartilage 75% repair of defect depth 50% repair of defect depth 25% repair of defect depth 0% repair of defect depth	4 3 2 1 0
Integration to Border Zone	Complete integration with surrounding cartilage Demarcating border < 1mm 3/4 of graft integrated, 1/4 with a notable border >1mm width 1/2 of graft integrated with surrounding cartilage,1/2 with a notable border > 1mm From no contact to 1/4 of graft integrated with surrounding cartilage	4 3 2 1 0
Macroscopic Appearance	Intact smooth surface Fibrillated surface Small, scattered fissures or cracks Several, small or few but large fissures Total degeneration of grafted area	4 3 2 1 0
Overall Score	Grade I normal Grade II nearly normal Grade III abnormal Grade IV severely abnormal	12 11-8 7-4 3-1